

Convolutional Neural Networks Based GNSS Signal Classification using Correlator-Level Measurements

Changhui Jiang¹, Yuwei Chen^{1*}, Bing Xu², Jianxin Jia¹, Haibin Sun¹, Zhe He³, Tinghuai Wang⁴ and Juha Hyyppä¹

1. Department of Photogrammetry and Remote Sensing, Finnish Geospatial Research Institute, Masala, FI-02430 Finland
2. Interdisciplinary Division of Aeronautical and Aviation Engineering, The Hong Kong Polytechnic University, Hong Kong
3. Department of Geomatics Engineering, University of Calgary
4. Huawei Helsinki Research Centre, Finland

Commission III, WG III/1

KEY WORDS: GNSS, NLOS, Multipath, Convolutional Neural Networks.

ABSTRACT:

In urban areas, the None-Line-Of-Sight (NLOS) and Multipath (MP) signals are the major issues degrading the GNSS position accuracy. Signal reception type should be identified before correcting the NLOS or MP induced errors. Signal features, i.e., signal strength, change rate of received signal strength, difference between delta pseudo-range and pseudo-range rate, have been explored in signal reception type classification. In this letter, with the aim to improve the signal classification accuracy, we propose a new GNSS NLOS/MP/LOS signals classification method using the correlator-level measurements. Firstly, vector tracking (VT) is employed to generate correlator-level measurements; secondly, a deep learning method, Convolutional Neural Network (CNN), is employed to automatically extract the features and identify the signal reception type, correlators' outputs calculated at different code phases are employed as the inputs of the CNN. Field test is carried out for assessing the performance of the proposed method, and the CNN method obtains state-of-art performance compared with the K-nearest Neighbors Algorithm (kNN) and Support Vector Machine (SVM) methods.

1. INTRODUCTION

With the booming of the Unmanned Ground Vehicles (UGV) and mobile Location Based Services (LBS), reliable position information is critical for these applications (Guo et al., 2014; Lohan et al., 2013; Cheng et al., 2020). Currently, Global Navigation Satellite System (GNSS) is the fundamental system for generating precise position, velocity and time information. Users with GNSS receivers can obtain precise navigation solutions while there are sufficient in-view satellites (Houranni et al., 2020; Jiang et al., 2020a; Jiang et al., 2020b). However, in urban areas, tall buildings will block the signals from the satellites with low elevation angles. Poor geometry distribution of the in-view satellites will degrade the estimation accuracy of the position accuracy across the road (Jiang et al., 2021; Cho et al., 2019; Xu et al., 2020; Yozevitch et al., 2016). Basically, there are three GNSS signal types in urban areas: Line-Of-Sight (LOS), Multipath (MP) and None-Line-Of-Sight (NLOS). LOS refers to the signals directly received by the GNSS receivers (Jiang et al., 2021; Cho et al., 2019; Xu et al., 2020; Yozevitch et al., 2016). MP means both direct and reflected signals are received or reflected signals with different time delay are received at the same time. NLOS means only reflected signals are received and the LOS signal is blocked. The NLOS or MP signal reception will induce additional errors in the pseudo range measurements, which ultimately degrades the navigation solutions estimation (Jiang et al., 2021; Cho et al., 2019; Xu et al., 2020; Yozevitch et al., 2016). NLOS and MP induced errors should be detected and corrected for guaranteeing the GNSS position accuracy especially in urban areas (Jiang et al., 2021; Cho et al., 2019; Xu et al., 2020; Yozevitch et al., 2016).

Generally, there are usually three steps to deal with the NLOS/MP reception: Classification, Mitigation and Correction. Classification is the premise of the mitigation and correction.

There are different types of the methods for classifying NLOS/MP/NLOS:

(1) The first method is built on the analysis of the attributes of the NLOS/MP/LOS signals, NLOS signal usually has lower signal strength due the signal reception by the surface of the surrounded buildings or objects (Jiang et al., 2021; Cho et al., 2019; Xu et al., 2020; Yozevitch et al., 2016). In addition, some other features, signal strength, change rate of received signal strength, difference between delta pseudo-range and pseudo-range rate etc., extracted from the signal strength, pseudo range and pseudo range rates are employed to classifying these signal types. Some machine learning methods, e.g., Support Vector Machine (SVM), Fuzzy logic approach and other classifiers, are constructed to classify NLOS/MP/LOS signals (Jiang et al., 2021; Cho et al., 2019; Xu et al., 2020; Yozevitch et al., 2016). These investigations preliminarily demonstrate that these manually selected features are effective for identifying NLOS/MP signals. NLOS or MP reception will induce different correlators results compared with that of LOS signals. Signal strength, pseudo-range and pseudo-range rate measurements are obtained from signal tracking results (Groves., 2011; Liu et al., 2021; Chen et al., 2021). Therefore, correlators' outputs as deeper measurements might contribute to superior classification performance of the NLOS/MP/LOS.

(2) Apart from NLOS/MP/LOS classification using the signal attributes, some other sensors, i.e., LiDAR, 3D Map and Fish-eye Camera etc., are utilized to sense the environment and help to identify the NLOS/MP/LOS signals (Kubelka et al., 2020; Chen et al., 2017; Zidan et al., 2020; Sánchez et al., 2016; Ng et al., 2019; Le., 2015). With fish-eye camera, sky mask of the surrounded environment can be extracted through processing the images. With an attitude and heading reference system (AHRS), the satellites are project to the fish-eye camera images and the satellites visibility is obtained (Kubelka et al., 2020; Chen et al., 2017; Zidan et al., 2020; Sánchez et al., 2016; Ng et

al., 2019; Le., 2015). With 3D map or LiDAR, satellites visibility can be predicted through comparing the elevation angle of the building boundaries and the satellites (Kubelka et al., 2020; Chen et al., 2017; Zidan et al., 2020; Sánchez et al., 2016; Ng et al., 2019; Le., 2015). Also, signal transmitting path can be extracted with the LiDAR or 3D map. However, 3D maps or LiDAR based GNSS signal tracing are computation intensive and they are not always available (Jiang et al., 2020c). A self-contained NLOS/MP/LOS signals classification method is preferable and more applicable. Conventional self-contained classification methods utilized the signal attributes as the features not the baseband signal processing results. In fact, in a GNSS receiver, the correlators' outputs present the essential characteristics of the received signals (Xu et al., 2019), utilizing deeper processing results might contribute to higher classification accuracy. Therefore, in this letter, correlator-level measurements from multiple correlators are employed as the inputs of a deep learning method, specifically, correlators outputs are processed by Convolutional Neural Network (CNN) for classifying NLOS/MP/LOS signals.

Reminder of this letter is organized as: Section II gives the signal propagation model and the VT correlators model; Section III presents the employed CNN; and then, field test, settings, CNN parameters, experimental results and analysis are listed, finally, we conclude the paper, some discussions and future works are also added in this letter.

2. MODEL AND METHOD

2.1 LOS/NLOS/MP Signal Model

As aforementioned, GNSS satellites broadcast navigation signals to the earth, the receiver with an antenna receives the signals and processes it. The received raw signals are amplified, down-converted and sampled, then, the intermediate frequency (IF) dataset can be processed for signal acquisition, tracking and navigation solutions determination. According to the literatures, the LOS/NLOS/MP signal propagation models are given by (Xu et al., 2019; Jiang et al., 2019):

$$y_{LOS}(i \cdot T_s) = A \cdot C(i \cdot T_s - \tau_0) \cos((\omega_{IF} + \omega_d) \cdot i \cdot T_s + \varphi_0) + \eta_{LOS}(i \cdot T_s) \quad (1)$$

$$y_{MP}(i \cdot T_s) = A \cdot C(i \cdot T_s - \tau_0) \cos((\omega_{IF} + \omega_d) \cdot i \cdot T_s + \varphi_0) + \alpha_{MP} \cdot A \cdot C(i \cdot T_s - \tau_0 - \tau_{MP}) \cos\{(\omega_{IF} + \omega_d) \cdot i \cdot T_s + \varphi_0\} \quad (2)$$

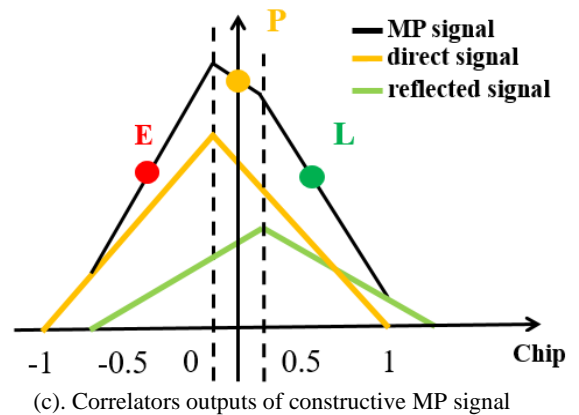
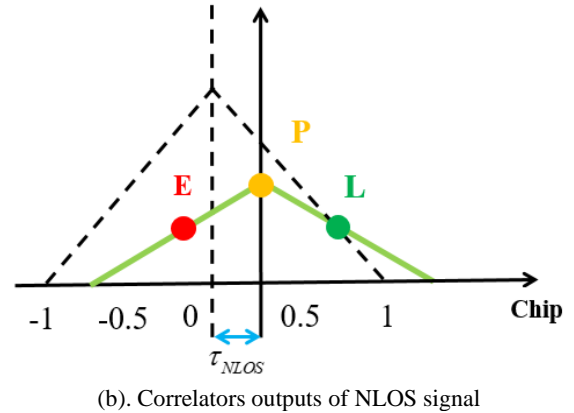
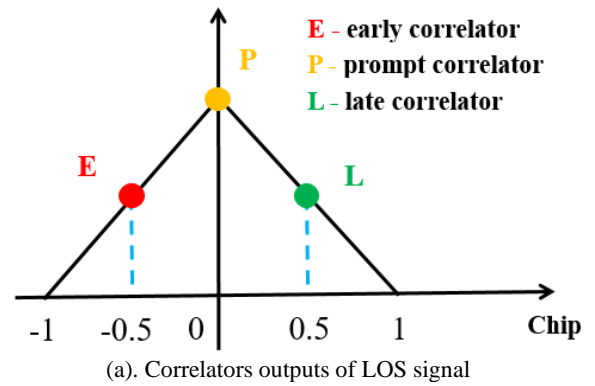
$$y_{NLOS}(i \cdot T_s) = \alpha_{NLOS} \cdot A \cdot C(i \cdot T_s - \tau_0 - \tau_{NLOS}) \cos\{(\omega_{IF} + \omega_d) \cdot i \cdot T_s + \varphi_0 + \Delta\varphi_{NLOS} + \Delta\omega_{NLOS} \cdot i \cdot T_s\} + \eta_{NLOS}(i \cdot T_s) \quad (3)$$

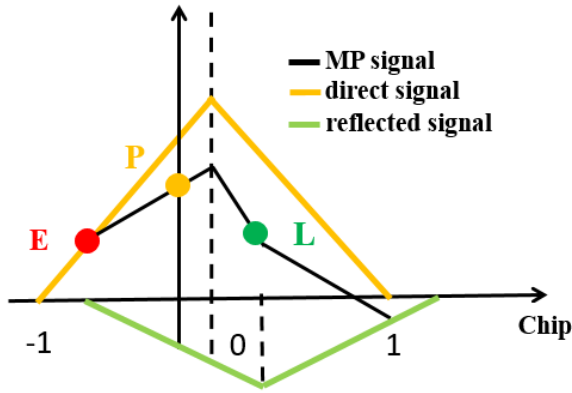
where T_s denotes the signal sampling duration, i denotes the index of the sampled signals; A denotes the amplitude of the LOS signal; $C(\cdot)$ denotes the pseudo-random noise code (PRN); τ_0 denotes the code phase delay of the LOS signals, τ_{MP} and τ_{NLOS} denote the NLOS or MP induced additional code phase delay; ω_{IF} denotes the frequency of the IF signal, ω_d is the Doppler shift; φ_0 is the carrier phase of the LOS signal, $\Delta\varphi_{MP}$ and $\Delta\varphi_{NLOS}$ are the additional carrier phase caused by the NLOS or MP signal reception; α_{MP} and α_{NLOS} are the coefficients of the MP and NLOS reflection; $\eta_{LOS}(i \cdot T_s)$, $\eta_{MP}(i \cdot T_s)$ and $\eta_{NLOS}(i \cdot T_s)$ are the additional Gaussian noise of the LOS, MP and NLOS signals respectively.

2.2 Correlators Measurements

In a typical GNSS receiver, signal tracking is accomplished by correlating the local signal replica and the incoming signal. The correlation results are employed to tune the parameters of the local signal replica generation. Usually, three local signal replicas, early (E), prompt (P) and late (L), with 0.5 code spacing are generated to correlate with the incoming signals for generate measurements. Following figure 1 illustrates the E, P, L correlators' outputs of the LOS, NLOS and MP signals (Xu et al., 2019). It can be seen that:

- (1) under LOS condition, the correlator peak is consistent with the prompt correlator, however, there is code phase bias between prompt correlator output and correlator peak under NLOS condition; in addition, the correlators magnitude is lower than that of LOS signal due to the power loss caused by the signal reflection.
- (2) under MP condition, the correlator peak is not consistent with prompt correlator, the correlators curves are not triangle due to the superposition of the LOS and reflected signals.





(d) Correlators outputs of destructive MP signal

Figure 1. Correlators outputs of the GNSS NLOS/MP/LOS signals (Xu et al., 2019; Jiang et al., 2022)

2.3 Preparation in electronic form

As presented in Section II.B, the correlators outputs curves are different for different signal receptions, which provides an opportunity to classify and identify NLOS/MP/LOS signals. Here, Convolutional Neural Networks (CNN) is designed and utilized to process the correlators outputs. Signal features are automatically extracted through the convolutional operation instead of manually selection in conventional methods. CNN structure is presented in figure 2, there are multiple layers between the input and output layers in the CNN, specifically, convolutional layers, Maxpooling layers and fully connected layers.

Firstly, the convolutional layers are utilized to extract the features of the inputs with the convolutional operation. Each convolutional layer employed multiple kernel functions to extract the features and characteristics. Assuming there are M_i kernel functions contained in the i_{th} convolutional layer. Kernel filter of the same convolutional layer utilizes the same kernel function to conduct the convolution operation of the input dataset. The convolutional layer operation equations are given by (Jiang et al., 2020a; Jiang et al., 2020b):

$$y_j^{(i)} = a \cdot \left(\sum_{r=1}^{M_k^{(i)}} w_r^{(i)} \cdot x_{r+j \times M_s^{(i)}} + b^{(i)} \right) \quad (4)$$

$$0 \leq j \leq \frac{M - M_k^{(i)}}{M_s^{(i)}}; \quad i = 1, 2, \dots, L \quad (5)$$

where the variable $M_k^{(i)}$ denotes the filters' kernel size, the variables $w_r^{(i)}$ and $b^{(i)}$ denote the weight and bias parameters of the kernel respectively, these parameters are optimized at the training phase.

Secondly, results of the convolutional layers are converted to an activation function, i.e., Sigmoid, Tanh, Rectified Linear Units (ReLU). According to the literatures, ReLU is the most popular activation function, and therefore, it is also selected as the activation function. After the convolutional layers, pooling layers are usually installed and employed to process the outputs from the convolutional layers. Through down-sampling and reducing the tensors' dimension from the convolutional outputs, the spatial reduction and computation load reduction are obtained. Pooling operation is conducted through selecting the maximum value in the current pooling window (MaxPooling). The convolutional and Maxpooling layers work together extract and learn the features of the inputs.

Finally, a fully connected layer is employed to generate and select the probability of the class with SoftMax function. Class with highest probability will be output as the classification result. Here, there are three labels for the CNN: NLOS, LOS and MP.

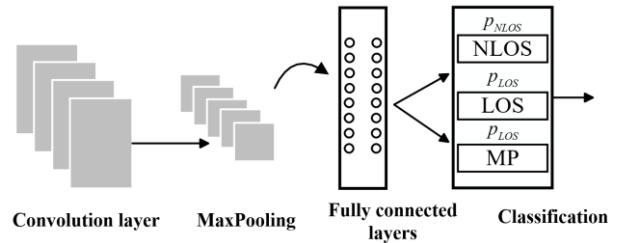
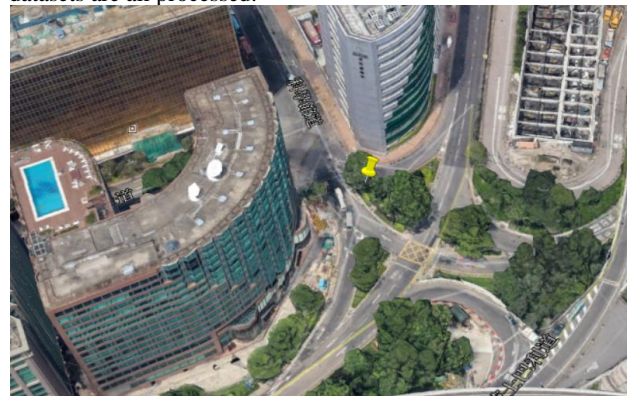


Figure 2. CNN structure for NLOS, LOS and MP classification

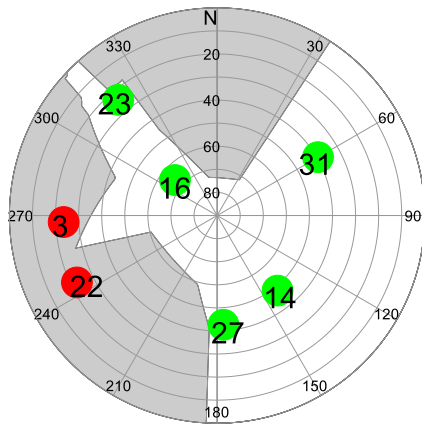
3. FIELD TEST AND RESULTS

3.1 Experimental Setting Up and Dataset Collection

With the aim to assess the performance of the proposed method for NLOS, LOS and MP classification, we carried out a field test and GPS L1 intermediate frequency (IF) dataset was collected. Figure 3(a) presents the GPS L1 dataset collecting site, the sampling frequency is 26 MHz and IF value is 0 MHz. More details of the signal collecting settings and hardware are presented in our recent paper (Xu et al., 2020). The signal collecting site is surrounded by tall buildings, and the satellites signals might be blocked or reflected by them. Figure 3(b) plots the sky mask extracted from 3D map and the ephemeris. Together with the signal processing results from a software defined receiver (SDR), PRN 3 and PRN 22 are NLOS signals, and PRN 23 and PRN 27 are multipath signals. In the experiment, we firstly process the collected GPS L1 IF dataset with a VT SDR, differently, multiple correlators with 0.01 code chip spacing are implemented for generating the correlators outputs curves (figure 1). Correlators curves are generated as the training dataset after being labeled through the satellite visibility extracted from 3D map and ephemeris. We collected another dataset in the same site after several minutes with the same settings. The second dataset is also processed by the VT SDR, and the correlators outputs are generated as the testing dataset. Considering the computation load brought by multiple correlators, therefore, 50 seconds of the training and testing datasets are all processed.



(a) GPS L1 IF dataset collecting site at a crossroad



(b) Sky visibility

Figure 3. GPS L1 IF signal dataset collection site in Google earth and the sky visibility plotting

3.2 CNN Classification Accuracy and Comparison

The outputs of the multiple correlators are directly employed by the CNN for extracting and learning features of different signals. The code phase ranged from -1 to 1 with 0.01 code chip spacing, therefore, the size of the CNN input vector was (1×200) . As aforementioned, the time length of the processed dataset is 50 seconds, then, each satellites could generate 50000 samples. Table 1 listed the details of the training and testing samples for each satellite, there are extracted from two different IF datasets processed by a same GNSS VT SDR. While accomplishing the CNN training, 10000 samples are selected from the testing dataset of each satellite. The selected samples are mixed and employed to evaluate the performance of the proposed method. NLOS/MP/LOS classification accuracy is presented in the Table 2, the CNNs with different layers are utilized in the classification with the aim to optimize the structure of the CNN. In the Table 2, Conv(a, b) refers to the CNN convolutional layer with a filters and the kernel size is b. For the Maxpooling (p, q) function, the variable p is the pooling size and q denotes the strides. With the classification results, it can be observed that:

(1) the CNN with two convolutional layers performs the highest classification accuracy in the dataset, while adding more layers after the Maxpooling function, the classification accuracy NLOS and LOS perform a little decrease, this phenomenon might indicate that two convolutional layers were sufficient for extracting the features for NLOS and LOS classification. However, the MP classification accuracy obtained a minor increase with another convolutional layer added after the Maxpooling function. The MP signals are more complex compared to NLOS and LOS, deeper CNN structure might help to increase the MP identification accuracy.

(2) LOS signals perform highest classification accuracy, MP signals perform the lowest classification accuracy, and, correlators' outputs of the NLOS/LOS signals are relatively easier to identify, MP correlators' outputs curves are more complex. MP signals are the mixture of the LOS and reflected signals, multiple code delays contribute to the complex curves of the correlators' outputs.

Table 1. Classification accuracy comparisons

PRN	Training samples	Testing samples	Label
3	40000	10000	NLOS
16	40000	10000	LOS
22	40000	10000	NLOS
23	40000	10000	MP
27	40000	10000	MP
31	40000	10000	LOS

PRN	Training samples	Testing samples	Label
3	40000	10000	NLOS
16	40000	10000	LOS
22	40000	10000	NLOS
23	40000	10000	MP
27	40000	10000	MP
31	40000	10000	LOS

Table 2. NLOS/LOS/MP classification accuracy

NLOS	MP	LOS	CNN
83.13%	79.47%	86.13%	Cov1D (2,2) MaxPooling (2,2)
87.82%	84.26%	89.82%	Cov1D (2,2) Cov1D (4,2) MaxPooling (2,2)
85.38%	84.91%	88.48%	Cov1D (2,2) Cov1D (4,2) MaxPooling (2,2) Cov1D (4,2)

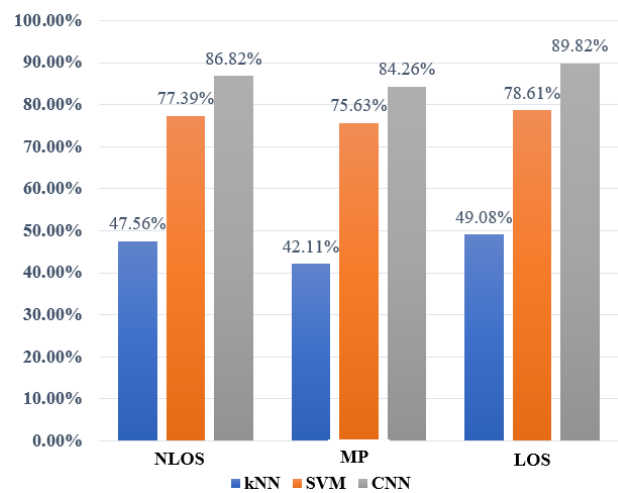


Figure 4. Classification accuracy comparison

We compare the CNN method with the manually selected features-based classifiers, i.e., kNN, SVM. Manually selected features, i.e., Signal noise ratio, Normalized pseudo range residual, are employed as the input features of the kNN and SVM classifier. Figure 4 presents the classification accuracy comparisons between the kNN, SVM and CNN. MP signals performs the lowest identification accuracy, and the LOS signals identification accuracy is the highest. CNN performs the best NLOS/MP/LOS classification accuracy.

3.3 Limitations and future work

Although the field-testing results preliminarily demonstrates the superiority of the CNN classifier using correlators' outputs, there are still some limitations degrading the classification accuracy.

(1) limited by the computation load, limited datasets are generated for training the CNN classifiers, much more labeled dataset must be helpful to improve the classification accuracy.

(2) the datasets are collected at the same site, the signals are reflected by the same target, if the testing dataset is collected from other sites, surfaces with different materials performs different reflection and refraction characteristics, which might

decrease the classification accuracy.

(3) there are abundant noises contained in the raw GNSS signals and the correlators' outputs, there is no de-noising operation for the correlators outputs in this letter. Suitable method de-noising the correlators outputs might be helpful to increase the classification accuracy.

We thought the following work is worth of further investigation.

(1) only CNN is employed as a deep learning method to investigate the GNSS signal classification, other advanced deep learning methods, i.e., Capsule Neural Network (Cap-NN), might outperforms than CNN.

(2) it is impossible to collect the datasets at everywhere, transfer learning should be considered to enhance the classifier versatility and generalization ability.

(3) restricted by the computation capacity, it is labor intensive to generate abundant training datasets, it is interesting to investigate Generative Adversarial Network or few-shot learning in this application.

CONCLUSIONS

In this paper, we firstly investigate a CNN based GNSS signal type classification directly with correlators outputs. In the CNN, GNSS correlators-level measurements are utilized as the inputs. Classification accuracy from different CNNs and machine learning methods are compared, and the field-testing results demonstrate the CNN with correlator-level measurements as the input have superior classification accuracy. In general, this letter at least supports the conclusion that deep learning method based GNSS signal classification using correlator-level measurement is an effective way. We firmly believe that our work has indicated a self-contained solution to improve the GNSS NLOS/MP/LOS signal classification, and it has potentials to be implemented in a mobile device, i.e., smartphone, to improve its GNSS position accuracy in urban areas.

REFERENCES

A. Al-Hourani and I. Guvenc, (2020). "On Modeling Satellite-to-Ground Path-Loss in Urban Environments," *IEEE Communications Letters*, 2020.

C. Jiang, S. Chen, Y. Chen, D. Liu and Y. Bo, (2020a). "An UWB Channel Impulse Response De-Noiseing Method for NLOS/LOS Classification Boosting," *IEEE Communications Letters*, vol. 24, no. 11, pp. 2513-2517, Nov. 2020.

C. Jiang, J. Shen, S. Chen, Y. Chen, D. Liu and Y. Bo (2020b). "UWB NLOS/LOS Classification Using Deep Learning Method," *IEEE Communications Letters*, vol. 24, no. 10, pp. 2226-2230, Oct. 2020.

C. Jiang, S. Chen, Y. Chen, D. Liu and Y. Bo, (2020c). "A GNSS Vector Tracking Method using Graph Optimization," *IEEE Transactions on Circuits and Systems II: Express Briefs*.

Jiang, C., Chen, S., Chen, Y., & Bo, Y. (2019). Research on a chip scale atomic clock aided vector tracking loop. *IET Radar, Sonar & Navigation*, 13(7), 1101-1106.

Chen, S., Zhou, B., Jiang, C., Xue, W., & Li, Q. (2021). A LiDAR/Visual SLAM Backend with Loop Closure Detection and Graph Optimization. *Remote Sensing*, 13(14), 2720.

Cho, S. J., Kim, B. S., Kim, T. S., & Kong, S. H. (2019). Enhancing GNSS Performance and Detection of Road Crossing

in Urban Area Using Deep Learning. *IEEE Intelligent Transportation Systems Conference (ITSC)*, pp. 2115-2120, 2019.

Chen, Y., Zhu, L., Tang, J., Pei, L., Kukko, A., Wang, Y., . . . Hyypää, H. (2017). Feasibility Study of Using Mobile Laser Scanning Point Cloud Data for GNSS Line of Sight Analysis. *Mobile Information Systems*.

E. S. Lohan and G. Seco-Granados, (2013). "C/N₀-Based Criterion for Selecting BOC-Modulated GNSS Signals in Cognitive Positioning," *IEEE Communications Letters*, vol. 17, no. 3, pp. 537-540, March 2013.

Jiang, C., Xu, B., & Hsu, L. T. (2021). Probabilistic approach to detect and correct GNSS NLOS signals using an augmented state vector in the extended Kalman filter. *GPS Solutions*, 25(2), 1-14.

Jiang, C., Chen, Y., Xu, B., Jia, J., Sun, H., Chen, C., ... & Hyypää, J. (2022). Vector Tracking Based on Factor Graph Optimization for GNSS NLOS Bias Estimation and Correction. *IEEE Internet of Things Journal*.

Groves, P. D. (2011). Shadow matching: A new GNSS positioning technique for urban canyons. *Journal of Navigation*, 64(3), 417-430.

Kubelka V, Dandurand P, Babin P, Giguère P, Pomerleau F, (2020). Radio propagation models for differential GNSS based on dense point clouds. *Journal of Field Robotics*, 1–16.

Zidan, J., Alluhaibi, O., Adegoke, E. I., Kampert, E., Higgins, M. D., & Ford, C. R. (2020). 3D Mapping Methods and Consistency Checks to Exclude GNSS Multipath/NLOS Effects. *IEEE International Conference on UK-China Emerging Technologies*, pp. 1-4.

Sánchez, J. S., Gerhmann, A., Thevenon, P., Brocard, P., Afia, A. B., & Julien, O. (2016). Use of a FishEye camera for GNSS NLOS exclusion and characterization in urban environments (2016).

Ng, H. F., Zhang, G., & Hsu, L. T. (2019). Range-based 3D mapping aided GNSS with NLOS correction based on skyplot with building boundaries. In *Proceedings of the ION Pacific PNT Meeting*, pp.737-751.

Le, Q. V. (2015). A tutorial on deep learning part 2: Autoencoders, convolutional neural networks and recurrent neural networks. *Google Brain*, 1-20.

Liu, D., Jiang, C., & Zhu, J. (2021). A gradient descend method - based none- line- of- sight- induced code delay searching in global navigation satellite system. *IET Radar, Sonar & Navigation*, 15(11), 1448-1457.

W. Guo, K. Yan, H. Zhang, X. Niu and C. Shi, (2014). "Double Stage NCO-Based Carrier Tracking Loop in GNSS Receivers for City Environmental Applications," *IEEE Communications Letters*, vol. 18, no. 10, pp. 1747-1750.

Xu, H., Angrisano, A., Gaglione, S., & Hsu, L. T. (2020). Machine learning based LOS/NLOS classifier and robust estimator for GNSS shadow matching. *Satellite Navigation*, 1, 1-12.

Yozevitch, R., Moshe, B. B., & Weissman, A, (2016). A robust GNSS los/nlos signal classifier. NAVIGATION: Journal of The Institute of Navigation, 63(4), 429-442, 2016.

Y. Cheng and Q. Chang, (2020). "A Carrier Tracking Loop Using Adaptive Strong Tracking Kalman Filter in GNSS Receivers," IEEE Communications Letters, 2020.